
LLM-DRIVEN MULTI-AGENT CURATION AND EXPANSION OF METAL-ORGANIC FRAMEWORKS DATABASE

Honghui Kim¹

ildmb96@kaist.ac.kr dhoonkim97@kaist.ac.kr jihankim@kaist.ac.kr

Dohoон Kim¹

Jihan Kim^{1*}

¹Department of Chemical and Biomolecular Engineering, Korea Advanced Institute of Science and
Technology, Daejeon, Republic of Korea

December 2, 2025

ABSTRACT

Metal-organic framework (MOF) databases have grown rapidly through experimental deposition and large-scale literature extraction, but recent analyses show that nearly half of their entries contain substantial structural errors. These inaccuracies propagate through high-throughput screening and machine-learning workflows, limiting the reliability of data-driven MOF discovery. Correcting such errors is exceptionally difficult because true repairs require integrating crystallographic files, synthesis descriptions, and contextual evidence scattered across the literature. Here we introduce LitMOF, a large language model-driven multi-agent framework that validates crystallographic information directly from the original literature and cross-validates it with database entries to repair structural errors. Applying LitMOF to the experimental MOF database (the CSD MOF Subset), we constructed LitMOF-DB, a curated set 118,464 computation-ready structures, including corrections of 69% (6,161 MOFs) of the invalid MOFs in the latest CoRE MOF database. Additionally, the system uncovered 12,646 experimentally reported MOFs absent from existing resources, substantially expanding the known experimental design space. This work establishes a scalable pathway toward self-correcting scientific databases and a generalizable paradigm for LLM-driven curation in materials science.

Keywords Material database · Metal-organic framework · Large language model · Multi-agent · Error correction

*Corresponding author

1 Introduction

Metal–organic frameworks (MOFs) constitute one of the most extensively studied classes of porous materials, with high structural diversity arising from the modular combination of metal nodes, organic linkers, and network topologies[1]. This diversity has motivated creation of large curated databases, including the CoRE MOF databases[2–4], the CSD MOF subset[5, 6], and MOSAEC-DB[7], which serve as the foundation for high-throughput simulations, machine learning based property prediction, and accelerated materials discovery [8, 9]. The accuracy and reliability of these databases are therefore central to all computational and data-driven MOF research.

However, recent work by White et al. revealed that structural errors are widespread across computation-ready MOF databases[10]. Using the metal oxidation state algorithm (MOSAEC), they reported that 51% of entries (>1.9 million structures) across 14 leading MOF databases violate basic chemical valence principles, and that 52% of top candidates in recent high-throughput screening studies are chemically invalid. Although several studies had previously noted the presence of structural inconsistencies[11–14], the scale of the issue had been significantly underestimated.

Current approaches to mitigate these errors, including the rule-based sanity checks[15], improved solvent removal workflows[4, 16], and MOSAEC curation pipeline[10], share a fundamental limitation in that they were designed to identify invalid structures, but not to repair them. Because these methods rely on fixed chemical rules and heuristic criteria, they cannot determine the correct structure when inconsistencies arise. As a result, large fractions of experimentally reported MOFs remain unusable for simulation. For example, in the latest CoRE MOF database[17], 7635 entries are designated as computation-ready, while 11,764 additional structures derived from the CSD fail to meet computational criteria after free-solvent removal[4]. This reflects the inherent difficulty of processing experimental CIFs into computation-ready CIFs. Moreover, MOFs reported in publications but not deposited as complete CIFs are excluded entirely, limiting coverage of the experimentally known space. Repairing these errors requires reconciling information scattered across multiple sources (e.g. original publications, crystallographic repositories, database records). But to date, performing this reconciliation manually for hundreds of thousands of structures has remained impossible.

To remedy this, we introduce LitMOF, the first LLM-driven multi-agent framework that can both detect and repair structural errors in experimental MOF entries by validating them against primary literature. LitMOF automatically retrieves evidence from (1) the literature (2) existing databases (CSD, CoRE MOF DB, MOSAEC-DB), and (3) crystallographic files, and cross-validates these resources to reconstruct chemically valid structures as originally synthesized and reported.

Applying this framework to 128,799 entries in the CSD MOF subset, we constructed LitMOF-DB, a corrected database of 118,464 valid MOFs. Notably, LitMOF-DB successfully recovers 69% (6,161 MOFs) of the non-computation-ready CoRE MOF structures (free solvent removed entries originated from CSD), demonstrating the ability of the framework to transform previously unusable structures into computation-ready form. Moreover, during the curation process, we identified 12,646 experimental MOFs present in the literature but absent from the CSD, further expanding the known experimental space.

Together, LitMOF and LitMOF-DB resolve long-standing issues of structural fidelity in MOF databases and provide a scalable pathway for incorporating missing experimental knowledge into computation-ready resources. This framework illustrates how LLM-powered agents can transform materials curation and lays the foundation for dynamic, self-correcting databases across diverse materials classes.

2 Results

2.1 LitMOF Agent Overview

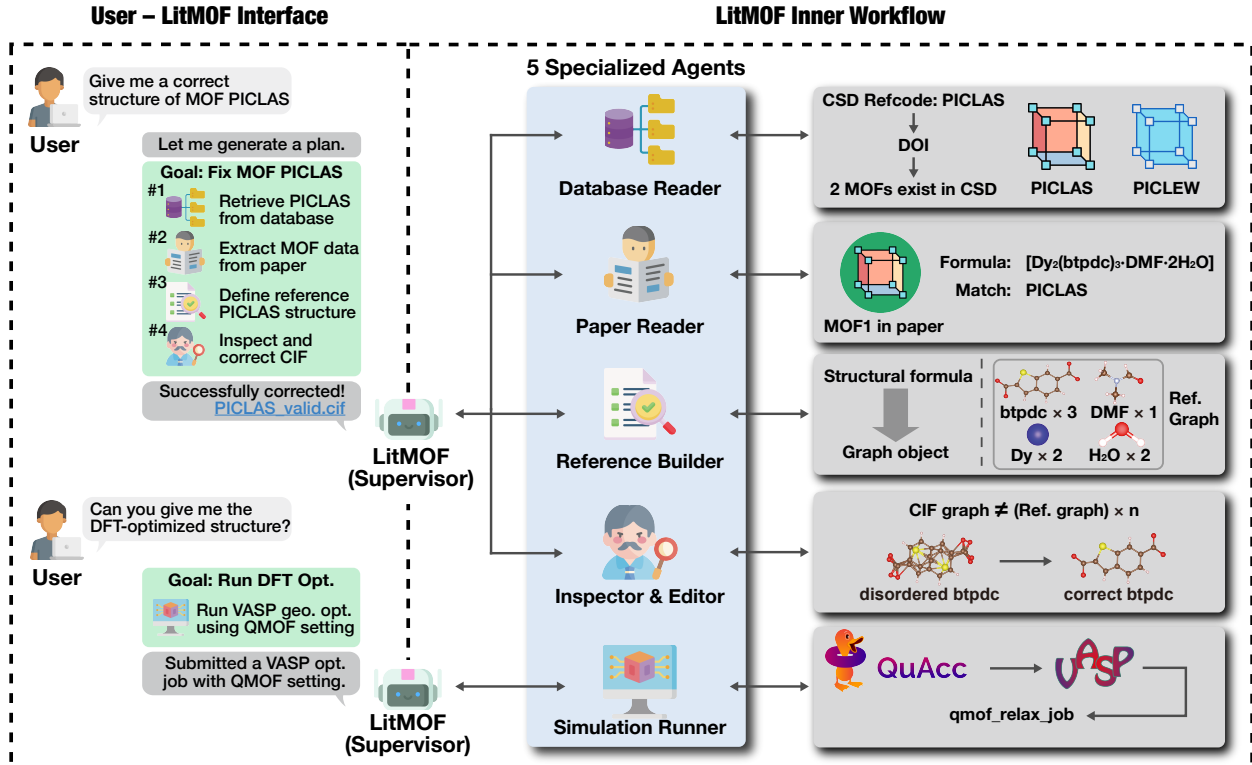


Figure 1: Schematic illustration of how LitMOF multi-agent system interacts with a user and generates responses. LitMOF consists of a Supervisor and five specialized agents, and the Supervisor interprets the user query and dispatches tasks to the appropriate agents. For the PICLAS example, LitMOF retrieves database records, extracts information from the publication, constructs a reference graph, and corrects structural errors in the CIF. LitMOF can also execute follow-up tasks, such as DFT geometry optimization, via the Simulation Runner.

Constructing large-scale databases requires workflows that can integrate information from diverse sources and correct structural inconsistencies automatically. Traditional automation has relied on hand-coded rules that operate only on structured data, whereas human experts routinely combine structured information with unstructured descriptions in publications to determine the correct MOF structure. To emulate this human-like reasoning, we developed LitMOF, a multi-agent system that leverages LLMs to automate the inspection and repair of structures.

The LitMOF system consists of a Supervisor together with five specialized agents: Database Reader, Paper Reader, Reference Builder, Inspector & Editor, and Simulation Runner. The Database and Paper Reader retrieve structural

information of MOFs from databases and publications. The Reference Builder constructs the expected structural motif from these sources, and the Inspector & Editor identifies and corrects inconsistencies and errors in the CIF. Finally, the Simulation Runner performs optional computational simulations on corrected structures. The Supervisor orchestrates all agents, maintains the execution plan, and interacts directly with the user.

Figure 1 illustrates the overall workflow. When a user requests the corrected structure of a MOF (e.g. CSD Refcode PICLAS), the Supervisor generates a plan that coordinates the four relevant agents: retrieving database records, extracting information from the associated publication, constructing the reference graph, and applying structural corrections. The validated structure is then returned to the user. In a second workflow, a user may request a DFT-optimized structure; in this case, the Supervisor includes the Simulation Runner, which prepares input files using the corrected CIF and submits a geometry optimization job. These examples highlight how LitMOF interprets user queries, decomposes the query into coordinated multi-agent tasks, and delivers corrected or computation-ready MOF structures. The detailed logic and plan-execution behavior of each agent are described in Section 2.3.

2.2 Plan-and-Execute Agent Architecture

The LitMOF system adopts a plan-and-execute agent architecture[18] in which every agent including the Supervisor and the five specialized agents follows a unified execution template (Figure 2a). Each agent is composed of a head module and a list of nodes, where a node may correspond to another agent responsible for a specific subtask or to an LLM/tool call that executes a well-defined function. The head module receives a query, generates or updates a plan, and determines the next node to execute. Powered by an LLM, the head module selects the next action based on the agent’s current state and the intermediate outputs produced during execution. Figure 2b illustrates representative scenarios in which the head module makes decisions. When an agent receives an external query, the head first interprets the query and generates an initial plan. If a plan already exists, the head module retrieves the current step from the plan and invokes the corresponding node. After the node is executed, the head receives the result, updates the plan accordingly, and determines the subsequent action. Throughout this process, the head module also decides when the plan is complete and when the agent should terminate and return a response. The plan consists of an overall goal to be achieved within the agent and an ordered list of subtasks, each represented by a node with its own description and execution status (see Figure 2c). During execution, the head sequentially selects the next node, invokes the associated function, records the result, and updates the plan status. This mechanism enables agents to operate autonomously while maintaining consistency across the entire system.

Because every agent follows the plan-and-execute style, the LitMOF system as a whole forms a hierarchical plan-and-execute architecture. Figure 2d illustrates the hierarchical structure of the plan-and-execute architecture using the workflow for correcting the MOF PICLAS as an example. When the Supervisor receives the user’s query, it generates a plan composed of coarse-grained tasks such as retrieving database records or extracting information from the publication. Each of these tasks is delegated to a specialized agent, which in turn generates its own plan consisting of finer-grained nodes tailored to its domain-specific function. For instance, the Paper Reader expands the Supervisor’s “extract MOF

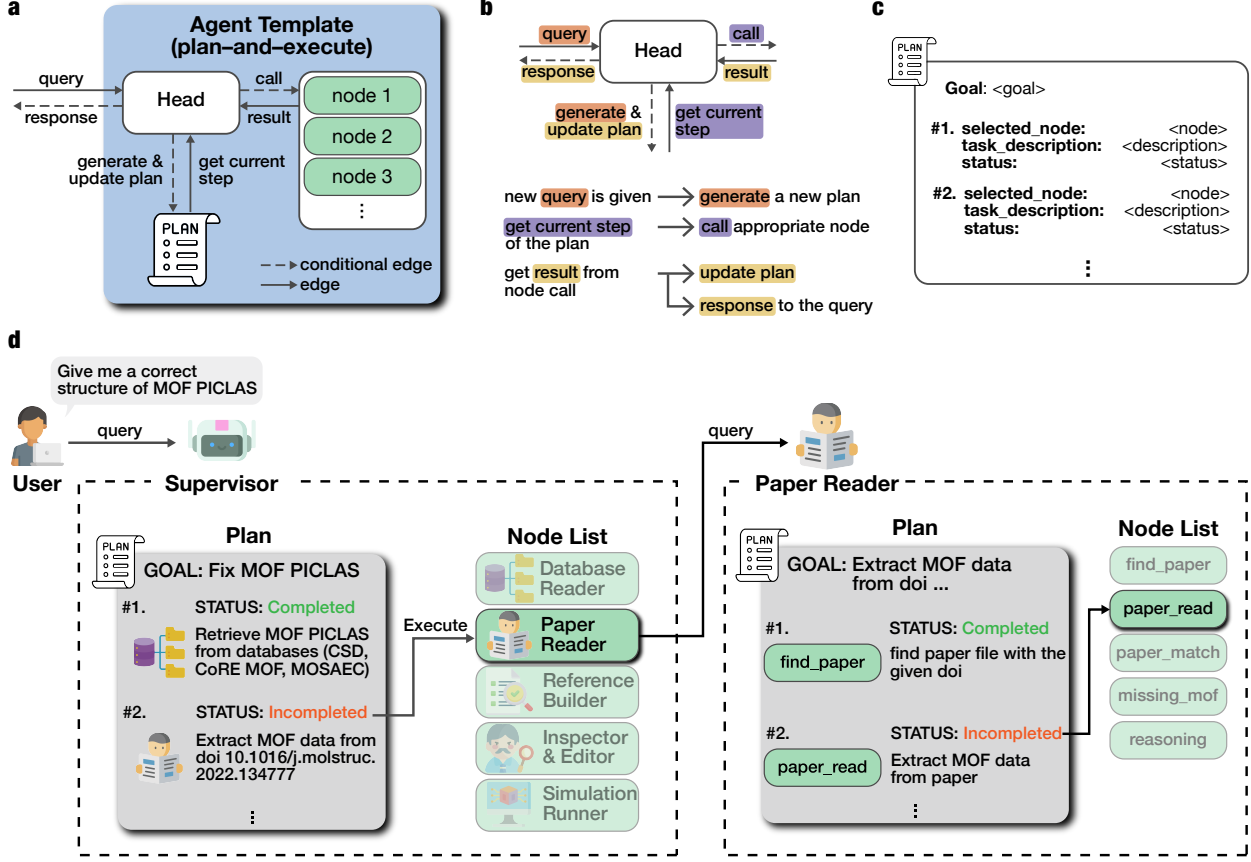


Figure 2: **a**, Unified agent template comprising an LLM-driven head module and a set of nodes, each representing either another agent call or an LLM/tool operation. **b**, Decision process of the head module, which interprets the query, generates or updates a plan, selects the next node, and determines termination. **c**, Structure of an agent plan, represented as a overall goal and an ordered list of nodes with associated descriptions and execution statuses. **d**, Hierarchical plan-and-execute behaviour illustrated using the PICLAS correction workflow, where the Supervisor’s high-level plan expands into finer-grained plans executed by specialized agents.

data from paper” task into subtasks such as locating the paper file, reading the paper, matching components, and resolving missing information. As each agent executes its plan and returns its results, the Supervisor integrates the outputs and advances the overall workflow. This nested structure enables LitMOF to decompose complex queries into coordinated, interpretable, and reusable multi-agent plans.

2.3 Specialized Agents in LitMOF

The Database Reader retrieves structural metadata from the CSD, CoRE MOF DB, and MOSAEC-DB. For CSD entries, it uses the CSD Python API to obtain information such as the DOI, chemical name, chemical formula, and lattice parameters. The full list of CSD metadata fields collected by the Database Reader is summarized in Table S1. For the CoRE MOF DB and MOSAEC-DB, the agent checks whether a CIF file corresponding to a given Refcode is available. In the PICLAS example (Figure 1), no CIF associated with the Refcode PICLAS exists in either CoRE MOF DB or MOSAEC-DB, whereas CSD contains a valid entry. From the CSD, the Database Reader first retrieves the DOI linked

to PICLAS and identifies all MOF structures reported under that DOI. For PICLAS’s DOI, two structures (PICLAS and PICLEW) are present, and metadata are collected for both entries to support downstream tasks in the Paper Reader.

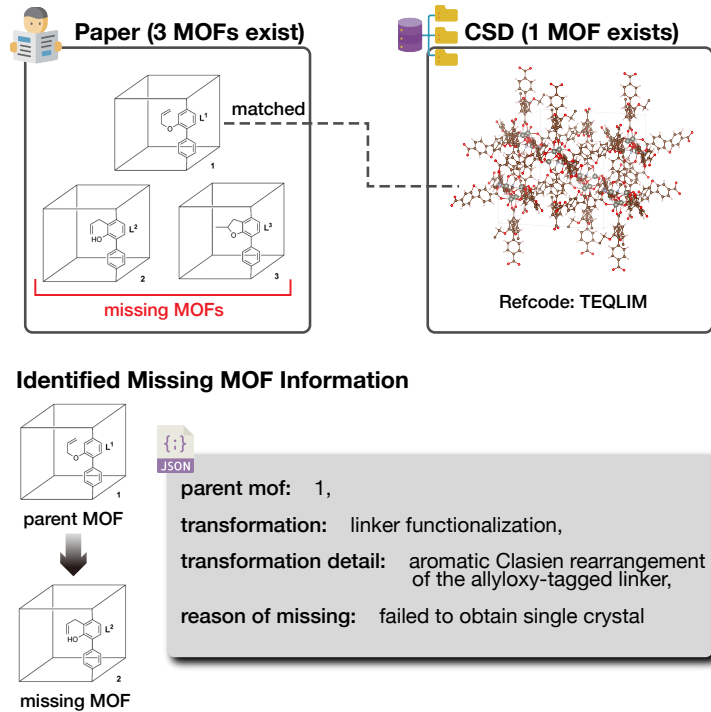


Figure 3: Example of a missing MOF case (refcode: TEQLIM). Missing MOFs refer to structures that were synthesized and characterized in the literature but were not deposited as CIF files in the CSD. This example contains two such missing MOFs. For each missing MOF, LitMOF identifies the parent MOF (the most structurally similar MOF available in the CSD), the transformation required to obtain the missing MOF from its parent, and the reason the CIF is missing when explicitly provided in the paper.

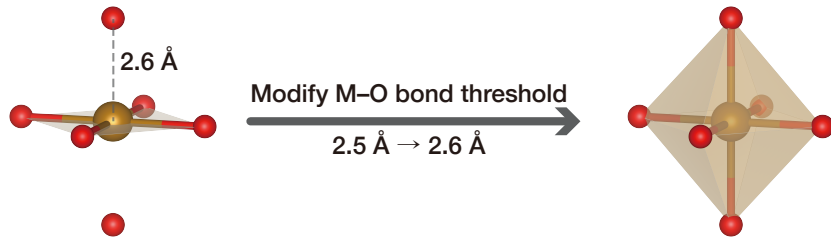
The Paper Reader identifies publications relevant to a given MOF and extracts structural and chemical information from the text. Its core functions include 1) locating paper file and parse the text, 2) extracting MOF specific metadata, 3) matching extracted information to CSD Refcodes, and 4) identifying missing MOFs that are synthesized but not deposited in CSD. List of extractable metadata from a paper is summarized in Table S4. In the PICLAS example, the Paper Reader first locates the publication using the DOI retrieved by the Database Reader. The identified file is then parsed to obtain cleaned text in either plain text or markdown format (a list of supported file formats and publishers is provided in Table S3). Using this parsed text, the Paper Reader extracts metadata for the two MOFs reported in the publication, including their structural formula, metal node, organic linker, solvent information, and physicochemical properties. These extracted MOFs are then matched to the two Refcodes, PICLAS and PICLEW, by comparing metadata obtained from the Database Reader and the Paper Reader. After matching, the agent optionally checks for MOFs that appear in the publication but do not correspond to any deposited CSD entry. We refer to these structures as missing MOFs. For each missing MOF, the agent identifies the most similar MOF among those with matched Refcodes (denoted as the parent MOF) and determines the transformation that converts the parent MOF into the missing MOF (see Figure 3).

The Reference Builder defines the expected reference structure of a MOF using information obtained from both the Database Reader and the Paper Reader. We define the reference structure as the minimal repeating unit of the MOF, which is typically described by its structural formula. In the PICLAS example, the structural formula extracted by the Paper Reader is $[\text{Dy}_2(\text{btpdc})_3 \cdot \text{DMF} \cdot 2(\text{H}_2\text{O})]$, indicating that the minimal repeating unit consists of two Dy atoms, three btpdc linkers, one DMF molecule, and two H_2O molecules. After determining this minimal repeating unit, the Reference Builder converts each component into a graph object. This transformation is supported by a combination of the PubChem API, an IUPAC name parser, and a predefined name to SMILES mapping. Because the Paper Reader provides expanded names for all abbreviations (for example, $\text{H}_2\text{btpdc} = \text{benzo[b]thiophene-2,6-dicarboxylic acid}$), the Reference Builder is able to generate complete structural graphs for all components, resulting in the final reference graph shown in Figure 1. The reference graph can be further validated and combined into a single graph object if CSD provides a valid chemical diagram of a MOF (see Figure S1).

The Inspector & Editor evaluates whether a CIF structure is consistent with the reference graph and corrects the structure when discrepancies are found. The agent first constructs a graph representation of the CIF. The source of CIF is either by using the CSD Python API or by parsing the provided CIF file. This CIF graph is then compared with the reference graph at several levels of structural detail to determine whether the structure is valid (see Figure S2). The first comparison assesses whether the species composition of the CIF follows the stoichiometric pattern encoded in the reference structure (see Figure S2a). This is examined by determining whether all atomic species in the CIF can be related to those in the reference structure through a single scaling factor. When all elements follow the same scaling factor, the overall species composition is regarded as consistent. If the species-level scaling pattern is consistent, the agent examines the coordination environment of atoms (see Figure S2b). The coordination environment is defined by the element type of the atom and the list of neighboring atoms' element types. Another direct comparison is to find subgraph that matches reference graph in the CIF graph (see Figure S2c).

Through these comparisons, the Inspector & Editor identifies three main categories of structural errors, which are bond errors, hydrogen errors, and unresolved disorder. Bond errors occur when the correct atoms are present, but the inferred bonding network does not match the reference connectivity. These errors are corrected by adjusting the bond-detection thresholds until the expected network is recovered (see Figure 4a). Hydrogen errors arise when the heavy-atom framework is correct, but hydrogen atoms are misplaced or missing. To address this issue, the agent identifies heavy-atom sites with incorrect hydrogen counts by comparing coordination-based identity labels or by matching the heavy-atom backbone of the reference graph to the corresponding subgraph in the CIF (see Figure 4b). Once the correct correspondence is established, hydrogen atoms are added or removed as needed. Unresolved disorder in CIF files results in duplicated fragments or multiple local configurations. When such disorder is detected, the agent enumerates all candidate structures consistent with the reference graph and evaluates their energies using a machine-learning interatomic potential (MLIP) trained on organic molecules, such as MACE-OFF24[19] (see Figure 4c). Unphysical candidates typically exhibit higher energies and are removed.

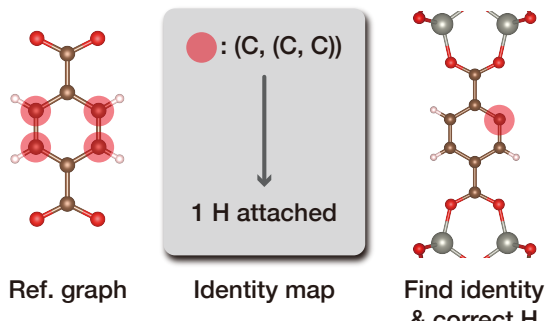
a Bond Correction



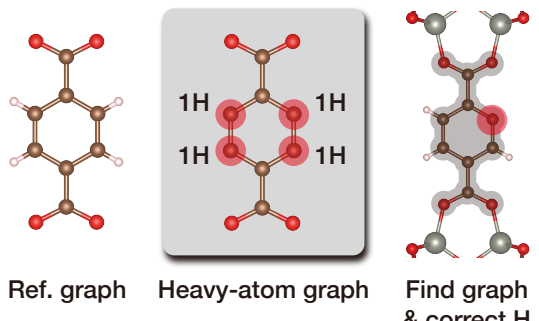
b Hydrogen Correction

[Identity Mapping]

Identity = (self, n^{th} heavy atom neighbors)



[Graph Matching]



c Disorder Correction

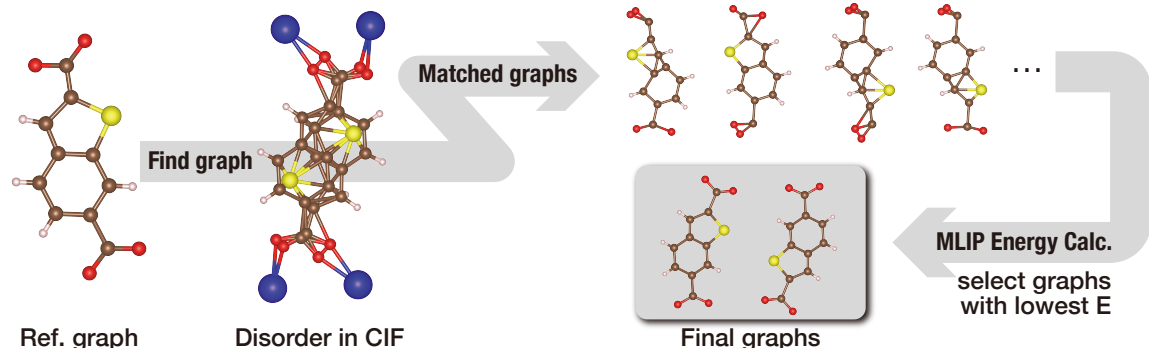


Figure 4: Three types of error correction handled by the Inspector & Editor agent. **a**, Bond errors are corrected by adjusting the distance threshold used to determine bond formation, which adds or removes bonds as needed. **b**, Hydrogen errors are corrected using two complementary methods, identity mapping and graph matching. **c**, Disorder correction resolves duplicated or entangled components into chemically meaningful configurations through graph matching and MLIP-based energy evaluation.

In the PICLAS example, the CIF graph fails the initial species count comparison test against the reference graph. The CIF graph contains the species counts {C: 176, H: 92, O: 80, S: 16, Dy: 8, N: 8}, whereas the reference graph contains {C: 33, H: 23, O: 15, S: 3, Dy: 2, N: 1}. The required repeating factor that aligns the Dy atom count between the two graphs is 4, which yields the scaled reference counts {C: 132, H: 92, O: 60, S: 12, Dy: 8, N: 4}. However, these values still do not match the CIF graph for C, O, S, and N, indicating that some components appear in excess.

relative to the expected minimal repeating unit. Such discrepancies suggest the presence of duplicated components arising from unresolved disorder in the CIF structure. This is further confirmed by sub-graph matching. Given that the minimal repeating unit (the reference graph) contains three btpdc linkers and one DMF molecule, a repeating factor of four implies that the CIF should contain twelve btpdc linkers and four DMF molecules. Instead, the CIF graph contains sixteen btpdc linkers and eight DMF molecules, demonstrating that both components are duplicated beyond their expected multiplicity. Therefore, the Inspector & Editor corrects the disorder, as illustrated in Figure 4c. During this process, the entangled btpdc site is disentangled into two possible configurations, resulting in multiple candidate CIF structures. To identify the most plausible configuration, we compute the energy of each candidate using a universal MLIP trained on materials (e.g., MACE-MPA-0[20]) and select the one with the lowest energy as the final corrected structure. The implications of having multiple correction solutions are further discussed in the Section 3.2.

Simulation Runner is a specialized agent that can run computational simulation or analysis tool on the corrected CIF. The agent can run density functional theory (DFT) simulation on the corrected CIF or analyze pore geometry of MOF structure using ZEO++ software[21]. DFT runs for MOF structures are powered by Quantum Accelerators package[22]. The Simulation Runner offers automatic simulation tools so that user can simultaneously correct structure and run simulation on the corrected structure. As illustrated in Figure 1, the Simulation Runner is called when user wants subsequent computational simulation on the corrected structure.

2.4 Construction of LitMOF-DB

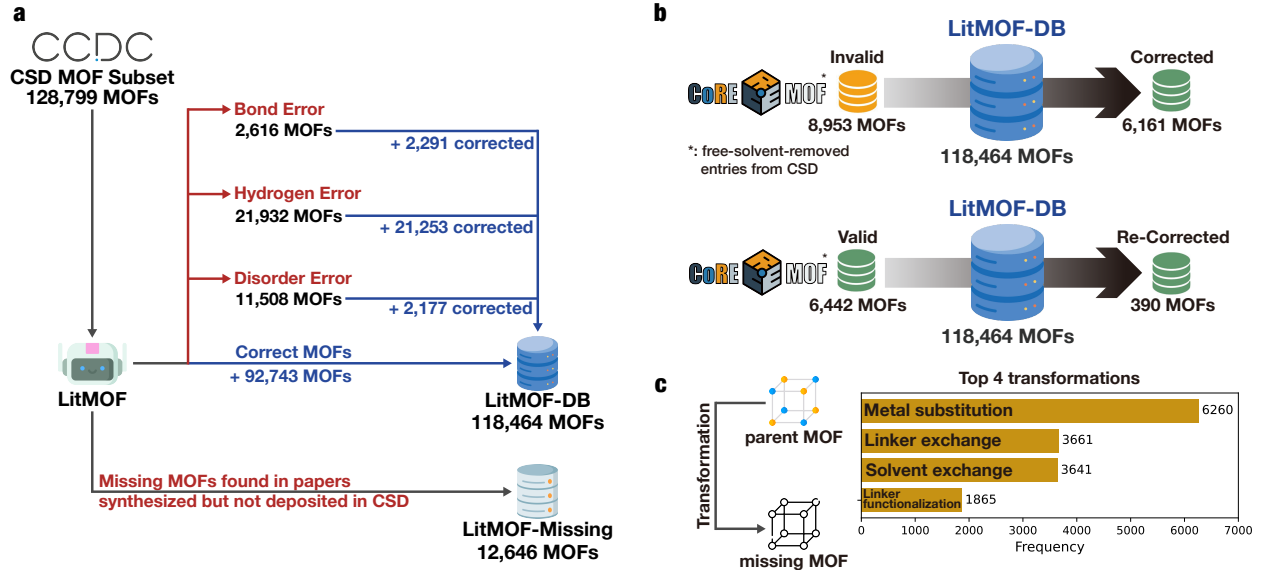


Figure 5: **a**, Results of the database construction using the LitMOF agent. Starting from the CSD MOF subset containing 128,799 structures, we corrected 25,721 MOFs and constructed a curated database of 118,464 experimental MOFs with free solvent removed. During this process, we also identified 12,646 missing MOFs and compiled a separate missing-MOF database. **b**, Comparison between our curated MOF database and the latest CoRE MOF database[17]. **c**, The four most common transformations that relate a parent MOF to its corresponding missing MOF.

We applied the automated database curation workflow to the CSD MOF subset, which contains 128,799 experimentally synthesized MOFs. These structures are linked to 53,306 publications, and among them we were able to access 36,146 papers from Elsevier, the American Chemical Society, the Royal Society of Chemistry, and Wiley. The exact counts for each publisher are summarized in Supporting Information. Using the LitMOF workflow, we constructed a curated and computation-ready database of 118,464 MOFs (Figure 5a). All solvent molecules were removed so that each MOF is provided as a computation-ready CIF. Across the full CSD MOF subset, we identified 2,616 cases of bond errors, 21,932 cases of hydrogen-placement errors, and 11,508 cases of disorder-related errors. A single MOF may contain more than one error type, but for analysis each MOF was assigned the most severe error type. LitMOF successfully corrected 2,291 bond-error structures (88%), 21,253 hydrogen-error structures (97%), and 2,177 disorder-error structures (19%). We compared our curation results with the latest CoRE MOF database[17]. Among the free-solvent-removed CoRE MOF entries that originate from the CSD, 6,442 structures are labeled as computation-ready (valid) and 8,953 structures as not computation-ready (invalid). Among the 8,953 structures classified as not computation-ready, our curated database corrected 6,161 MOFs (69%). In addition, we identified 390 structures (6%) that had been labeled as computation-ready but were false positives, and corrected them in the process of building the curated database (Figure 5b).

From the output of the Paper Reader during the database construction, we identified 12,646 missing MOFs. These are MOFs that were synthesized and characterized in the original publications but for which no CIF file was deposited in the CSD. For each missing MOF, the Paper Reader determines the corresponding parent MOF, defined as the most similar MOF structure in the paper, and extracts the transformation that relates the parent structure to the missing one. If the publication provides an explanation for the absence of a deposited CIF, this information is also recorded. The most common types of transformations include metal substitution, linker exchange, solvent exchange, and linker functionalization. When possible, we generate new CIF files for the missing MOFs by applying the extracted transformation to the parent MOF. These generated CIFs represent experimentally synthesized structures, although the atomic positions introduced by the transformation are not experimentally validated through techniques such as X-ray diffraction. Regardless of whether a CIF can be generated, the identification of missing MOFs significantly expands the available information on experimentally reported MOFs and enriches the overall dataset.

3 Discussion

3.1 Bond Corrected CIF

Previous computation-ready MOF databases typically discard bond information, so most CIF files in these databases do not contain a usable bond network. Simulation workflows usually do not require explicit bond definitions, but many structure processing tasks depend critically on them. Examples include metal node decomposition, organic linker decomposition, and defect generation. Distance based bond assignment algorithms are commonly used to reconstruct the bond network, yet these methods frequently overestimate or underestimate bonds because MOF bonding environments

and periodic structures are highly diverse. As a result, the reconstructed bond networks are often inaccurate and lead to failures in later structural analysis and modification.

LitMOF-DB resolves this issue by providing CIF files with validated and corrected bond information. As shown in Figure 4a, we apply a bond correction procedure that identifies and fixes wrong bonds while taking periodic boundary conditions and unit cell vectors into account. The CIF files in LitMOF-DB therefore contain a consistent bond network suitable for structure processing and advanced MOF analysis.

3.2 Multiple Solutions for Correction

Certain MOF structures admit multiple valid solutions during the correction process. Such non-unique outcomes occur most often in hydrogen correction and disorder corrections and arise from the inherent limitations of unitcell representations rather than from the LitMOF workflow itself. Hydrogen atoms are too light to be located reliably through X-ray diffraction or similar crystallographic techniques, so their positions are typically assigned during post-processing. Our hydrogen-correction procedure follows the same principle. However, post-processed hydrogen placement does not always have a unique solution. For example, when a linker contains a carboxylic acid group that is not coordinated to a metal center and the CIF lacks hydrogen atoms on the oxygen sites, a hydrogen atom must be placed on one of the two oxygens. Either placement is chemically reasonable, and in a MOF with several such groups, the number of valid configurations increases rapidly. Since crystallographic data cannot distinguish between these possibilities, we select the configuration with the lowest predicted energy. To manage the potentially large configuration space, we use a foundational MLIP trained on materials to evaluate the candidate structures efficiently. This approach identifies the most stable hydrogen assignment while keeping the computational cost manageable. For well-established structural motifs, such as the μ_3 -OH and μ_3 -O groups in Zr₆ metal node, predefined chemical rules are applied to reduce ambiguity and further improve the accuracy of the correction.

Disorder correction follows a similar rationale. Properly resolved disorder in a CIF does not pose any difficulty, but unresolved disorder results in duplicated atoms with fractional occupancies, which prevents the structure from being used reliably in computational simulations. This situation arises when a portion of the structure has intrinsic degree of freedom in rotation or has specific orientation, so the experimentally supported atomic position cannot be represented by a single configuration in the CIF. Such dynamic disorder commonly occurs in rotatable organic linkers, functionalized linkers, and weakly bound solvent molecules. Our disorder correction procedure decomposes these fractional and spatially ambiguous sites into a set of distinct and chemically meaningful configurations. As illustrated in Figure 4c, the meaningful selected configurations can be multiple. Static disorder, where an atom is replaced by a specific element during correction, can also produce multiple plausible outcomes. During database construction, we selected the lowest energy configuration using the same strategy applied in hydrogen correction. However, if requested, the agent can return all possible configurations rather than a single representative structure.

4 Conclusion

In this work, we introduced LitMOF, an LLM-driven multi-agent framework that automatically retrieves, interprets and reconciles information from the literature, crystallographic databases, and CIF files to repair structural errors in MOFs. Applied to the CSD MOF subset, LitMOF produced LitMOF-DB, a curated collection of 118,464 computation-ready experimental MOFs that resolves long-standing issues of hydrogen placement, bond inconsistencies, and unresolved disorder. The framework successfully corrected the majority of non-computation ready CoRE MOF structures and identified 12,646 experimentally synthesized but previously undocumented MOFs by extracting structural information directly from the literature.

These results demonstrate that LLM-powered agents can perform multi-source reasoning at scale, restoring structural fidelity and expanding coverage beyond what conventional rule-based workflows can achieve. More broadly, LitMOF provides a generalizable approach for building dynamic, self-correcting materials databases by integrating structured repositories with unstructured scientific text. As LLM capabilities continue to advance, such agentic systems are poised to play an increasingly central role in automated materials curation, simulation, and discovery.

Acknowledgment

This work acknowledge funding from the National Research Foundation of Korea under project number of RS-2024-00435493.

References

- [1] Omar M Yaghi, Michael O’Keeffe, Nathan W Ockwig, et al. “Reticular synthesis and the design of new materials”. In: *Nature* 423.6941 (2003), pp. 705–714.
- [2] Yongchul G Chung, Jeffrey Camp, Maciej Haranczyk, et al. “Computation-ready, experimental metal–organic frameworks: A tool to enable high-throughput screening of nanoporous crystals”. In: *Chemistry of Materials* 26.21 (2014), pp. 6185–6192.
- [3] Yongchul G Chung, Emmanuel Haldoupis, Benjamin J Bucior, et al. “Advances, updates, and analytics for the computation-ready, experimental metal–organic framework database: CoRE MOF 2019”. In: *Journal of Chemical & Engineering Data* 64.12 (2019), pp. 5985–5998.
- [4] Guobin Zhao, Logan M Brabson, Saumil Chheda, et al. “CoRE MOF DB: A curated experimental metal-organic framework database with machine-learned properties for integrated material-process screening”. In: *Matter* 8.6 (2025).
- [5] Frank H Allen. “The Cambridge Structural Database: a quarter of a million crystal structures and rising”. In: *Structural Science* 58.3 (2002), pp. 380–388.
- [6] Peyman Z Moghadam, Aurelia Li, Seth B Wiggin, et al. “Development of a Cambridge Structural Database subset: a collection of metal–organic frameworks for past, present, and future”. In: *Chemistry of materials* 29.7 (2017), pp. 2618–2625.
- [7] Marco Gibaldi, Anna Kapeliukha, Andrew White, et al. “MOSAEC-DB: a comprehensive database of experimental metal–organic frameworks with verified chemical accuracy suitable for molecular simulations”. In: *Chemical Science* 16.9 (2025), pp. 4085–4100.
- [8] Yeonghun Kang, Hyunsoo Park, Berend Smit, and Jihan Kim. “A multi-modal pre-training transformer for universal transfer learning in metal–organic frameworks”. In: *Nature Machine Intelligence* 5.3 (2023), pp. 309–318.
- [9] Gianmarco G Terrones, Shih-Peng Huang, Matthew P Rivera, et al. “Metal–organic framework stability in water and harsh environments from data-driven models trained on the diverse WS24 data set”. In: *Journal of the American Chemical Society* 146.29 (2024), pp. 20333–20348.
- [10] Andrew J White, Marco Gibaldi, Jake Burner, R Alex Mayo, and Tom K Woo. “High Structural Error Rates in “Computation-Ready” MOF Databases Discovered by Checking Metal Oxidation States”. In: *Journal of the American Chemical Society* 147.21 (2025), pp. 17579–17583.
- [11] Sadiye Velioglu and Seda Keskin. “Revealing the effect of structure curations on the simulated CO₂ separation performances of MOFs”. In: *Materials Advances* 1.3 (2020), pp. 341–353.
- [12] Hilal Daglar, Hasan Can Gulbalkan, Gokay Avci, et al. “Effect of metal–organic framework (MOF) database selection on the assessment of gas storage and separation potentials of MOFs”. In: *Angewandte Chemie International Edition* 60.14 (2021), pp. 7828–7837.

- [13] Taoyi Chen and Thomas A Manz. “Identifying misbonded atoms in the 2019 CoRE metal–organic framework database”. In: *RSC advances* 10.45 (2020), pp. 26944–26951.
- [14] Marco Gibaldi, Ohmin Kwon, Andrew White, Jake Burner, and Tom K Woo. “The HEALED SBU library of chemically realistic building blocks for construction of hypothetical metal–organic frameworks”. In: *ACS Applied Materials & Interfaces* 14.38 (2022), pp. 43372–43386.
- [15] Xin Jin, Kevin Maik Jablonka, Elias Moubarak, Yutao Li, and Berend Smit. “MOFChecker: a package for validating and correcting metal–organic framework (MOF) structures”. In: *Digital Discovery* (2025).
- [16] Marco Gibaldi, Anna Kapeliukha, Andrew White, and Tom K Woo. “Incorporation of ligand charge and metal oxidation state considerations into the computational solvent removal and activation of experimental crystal structures preceding molecular simulation”. In: *Journal of Chemical Information and Modeling* 65.1 (2024), pp. 275–287.
- [17] Guobin Zhao, Logan M. Brabson, Saumil Chheda, et al. *Computation-Ready Experimental Metal-Organic Framework (CoRE MOF) 2024 Dataset*. Version 1.1. Zenodo, Mar. 2025. doi: 10.5281/zenodo.15055758. URL: <https://doi.org/10.5281/zenodo.15055758>.
- [18] Lei Wang, Wanyu Xu, Yihuai Lan, et al. “Plan-and-solve prompting: Improving zero-shot chain-of-thought reasoning by large language models”. In: *arXiv preprint arXiv:2305.04091* (2023).
- [19] Dávid Péter Kovács, J Harry Moore, Nicholas J Browning, et al. “Mace-off: Short-range transferable machine learning force fields for organic molecules”. In: *Journal of the American Chemical Society* 147.21 (2025), pp. 17598–17611.
- [20] Illyes Batatia, Philipp Benner, Yuan Chiang, et al. “A foundation model for atomistic materials chemistry”. In: (2023). arXiv: 2401.00096 [physics.chem-ph].
- [21] Thomas F Willems, Chris H Rycroft, Michaeel Kazi, Juan C Meza, and Maciej Haranczyk. “Algorithms and tools for high-throughput geometry-based analysis of crystalline porous materials”. In: *Microporous and Mesoporous Materials* 149.1 (2012), pp. 134–141.
- [22] Andrew Rosen. *quacc – The Quantum Accelerator*. Version v1.0.6. Oct. 2025. doi: 10.5281/zenodo.17373420. URL: <https://doi.org/10.5281/zenodo.17373420>.

Supporting Information

LLM–Driven Multi-Agent Curation and Expansion of Metal–Organic Frameworks Database

Honghui Kim¹, Dohoон Kim¹, Jihan Kim^{1*}

¹Department of Chemical and Biomolecular Engineering, Korea Advanced Institute of Science and Technology, Daejeon, Republic of Korea

Supplementary Note S1. Methods

All agents and tools in LitMOF use the Mistral Small 3.2 Instruct (24B) model as core LLM. Without quantization, the model fits on a single NVIDIA A100 80 GB GPU. For text extraction from PDF files, which requires optical character recognition, we employ the DeepSeek-OCR vision–language model. Given a PDF file, DeepSeek-OCR produces a structured markdown representation that can be directly provided as input to the LLM.

Table S1: List of metadata fields retrieved from the Cambridge Structural Database (CSD) by the Database Reader agent.

Field	Description
chemical_name	Chemical name of the MOF structure.
formula	Chemical formula.
synonyms	Alternative names or identifiers.
crystal_information.crystal_system	Crystal system (e.g., monoclinic, cubic).
crystal_information.space_group	Space group symbol.
crystal_information.cell_length_a,b,c	Unit cell edge lengths (a, b, c).
crystal_information.cell_angle_alpha,beta,gamma	Unit cell angles (α, β, γ).
crystal_information.volume	Unit cell volume (\AA^3).
has_disorder	Whether the structure contains disorder.
disorder_details	Detailed description of disorder, if available.
remarks	Additional remarks or comments.

Table S2: List of nodes of each specialized agent.

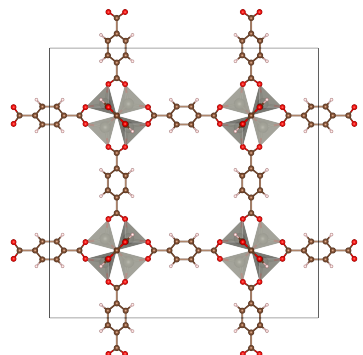
Agent	Node	Description
Database Reader	csd_retrieval_node	retrieve data from CSD database
	coremof_retrieval_node	retrieve data from CoRE MOF database
	mosaec_retrieval_node	retrieve data from MOSAEC-DB database
Paper Reader	find_paper_node	find paper file and parse the textual information of the paper into a string object
	paper_read_node	read a paper and extract all synthesized MOFs information
	paper_match_node	find a mapping between the extracted MOF information from a paper with relevant CSD reference code
	paper_missing_mof_node	find missing MOFs from a paper, that is synthesized but not deposited in CSD database
	reasoning_node	reasoning previous process result and find out mistakes.
Reference Builder	name_to_structure_node	transform chemical name into graph object using PubChem API, IUPAC name parser, and pre-defined list of name-SMILES mapping
	build_ref_graph_node	build reference graph by using the graph objects and CSD chemical diagram of a MOF
Inspector & Editor	diagnose_node	check a MOF whether it violates the reference graph
	correct_bond_node	correct bond error
	correct_hydrogen_node	correct hydrogen error
	correct_disorder_node	correct disorder error
Simulation Runner	dft_optimization_node	run DFT geometry optimization job
	dft_single_point_node	run DFT single point job
	pore_analysis_node	run ZEO++ to analyze pore geometry

Table S3: List of supported file formats and publishers.

Publisher	Supported File Format	Process Method
Elsevier	XML	Parser
Royal Society of Chemistry	HTML	Parser
American Chemical Society	XML	Parser
Wiley	PDF	Vision Language Model
International Union of Crystallography	PDF	Vision Language Model

Table S4: Metadata fields extracted by the Paper Reader agent from scientific publications.

Field group	Key	Description
Paper information	paper_info.MOF*.identifier_in_text	Label used for the MOF in the text (e.g., “1-Ln”, “1-Eu”).
	paper_info.MOF*.structural_formula	Structural formula as reported in the paper.
	paper_info.MOF*.chemical_formula	Chemical formula of the MOF.
	paper_info.MOF*.crystal_system	Crystal system (e.g., triclinic, monoclinic).
	paper_info.MOF*.space_group	Space group symbol.
	paper_info.MOF*.cell_parameters	Unit-cell parameters (a , b , c , α , β , γ).
	paper_info.MOF*.volume	Unit-cell volume.
	paper_info.MOF*.metal_node	Composition of the metal node (e.g., Eu, Tb, or mixture).
	paper_info.MOF*.metal_oxidation_state	Oxidation state of the metal node(s).
	paper_info.MOF*.organic_linker	Name and formula of the organic linker.
	paper_info.MOF*.solvent	Main solvent(s) used in synthesis or structure description.
Match information	paper_info.important_notes	Remarks on structure or properties (e.g., luminescence, applications).
	paper_info.abbreviations[*]	Dictionary mapping abbreviations (e.g., H2L, DMA) to full names.
Missing MOFs	match_info[refcode]	Mapping between a CSD refcode (e.g., GAZDEU) and its corresponding MOF ID (e.g., MOF3).
Missing MOFs	missing_mofs.MOF*.identifier_in_text	Label of a MOF mentioned in the paper but absent from structural databases.
	missing_mofs.MOF*.parent_mof	Parent MOF entry used as the structural reference.
	missing_mofs.MOF*.transformation	Type of transformation from the parent MOF (e.g., metal substitution).
	missing_mofs.MOF*.transformation_details	Description of how the missing MOF differs from its parent structure.
	missing_mofs.MOF*.reason_no_cif	Reason for the absence of a CIF file, if provided.

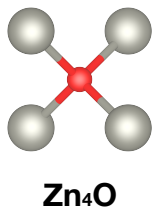


MOF-5
(Refcode: SAHYOQ)

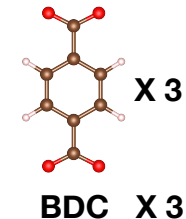
Structural formula: $\text{Zn}_4\text{O}(\text{BDC})_3$

BDC = 1,4-benzenedicarboxylate

Reference Graph Type 1

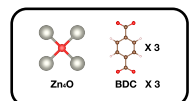


Zn_4O



$\text{BDC} \times 3$

Reference Graph Type 2

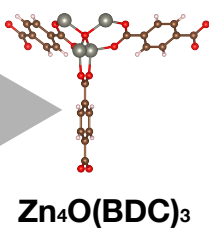


Ref. Graph Type 1

+

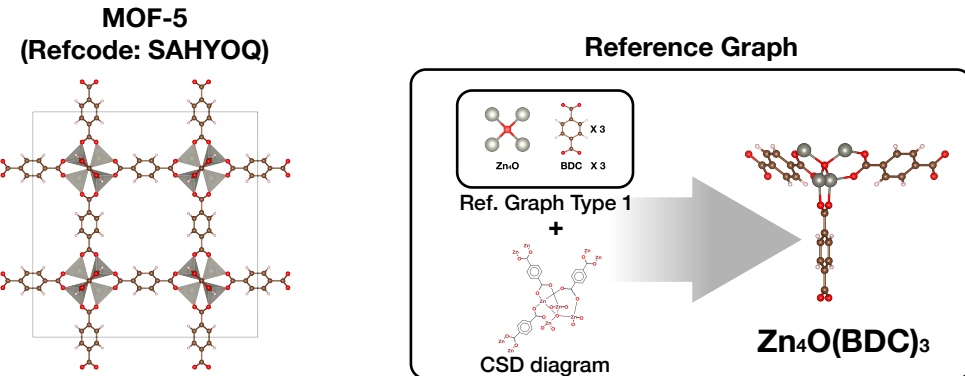


CSD diagram



$\text{Zn}_4\text{O}(\text{BDC})_3$

Figure S1: Two types of reference graph.



a. Species Count

Ref. Graph = {C: 24, O: 13, H: 12, Zn: 4 }
 CIF Graph = {C: 192, O: 104, H: 96, Zn: 32}

Ratio = {C: 8, O: 8, H: 8, Zn: 8 }

PASS. All species have same ratio between Ref. graph and CIF graph

b. Coordination Environment Count

Coord. Env.	Ref. Graph	CIF Graph
(Zn, (O, O, O, O)):	4	32
(O, (Zn, Zn, Zn, Zn)):	1	8
(O, (C, Zn)):	12	96
(C, (C, O, O)):	6	48
(C, (C, C, C)):	6	48
(C, (C, C, H)):	12	96
(H, (C)):	12	96

PASS. All coordination environment have same ratio between Ref. graph and CIF graph

c. Subgraph Matching

In CIF graph, 8 Zn₄O metal node and 24 BDC linker graphs are found.
 The ratio matches the ratio of reference graph (= 1:3).
PASS.

Figure S2: Three types of comparison test between reference graph and CIF graph.

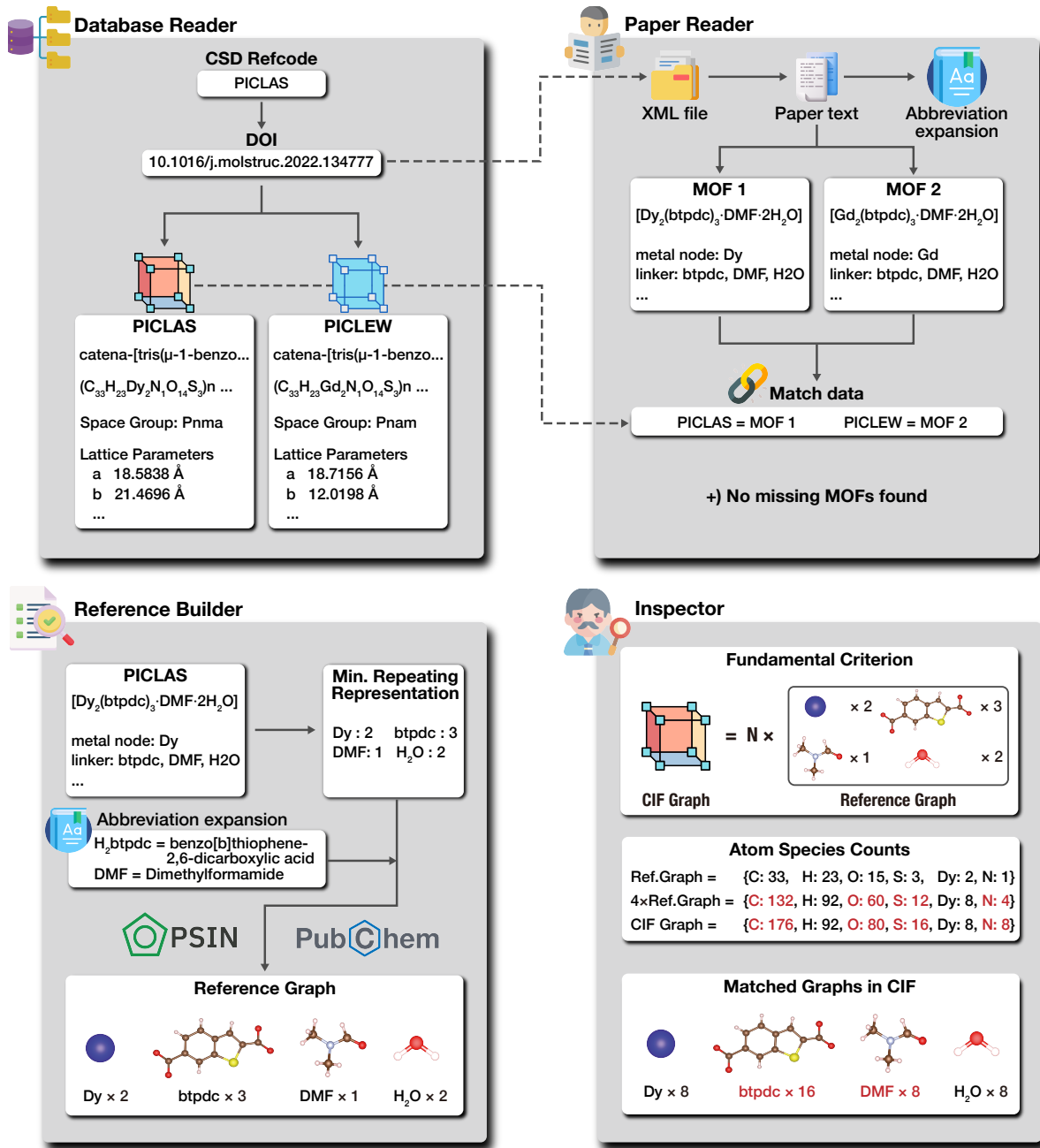


Figure S3: Detailed illustration of how LitMOF retrieves data for the example MOF PICLAS using the Database Reader and Paper Reader, constructs the reference graph using the Reference Builder, and identifies structural errors during inspection of the Inspector & Editor.